

A Polyelectrolyte Bearing Metal Ion Receptors and Electrostatic Functionality for Layer-by-Layer Self-Assembly

*Henning Krass, Georg Papastavrou, Dirk G. Kurth**

Max Planck Institute of Colloids and Interfaces, Research Campus Golm, 14424
Potsdam, Germany
Tel: +49 331-567 9211; Fax: +49 331-567 9202
E-mail: kurth@mpikg-golm.mpg.de

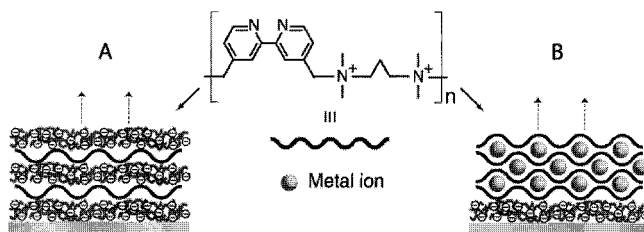
Summary: A polyelectrolyte (BiPE) containing bipyridine ligands as metal ion receptors and quaternary ammonium groups is described, which can be assembled via electrostatic interactions or metal ion coordination. Electrostatic layer-by-layer self-assembly of BiPE with sodium poly(styrene sulfonate) (PSS) as oppositely charged component results in striated multilayers. The BiPE/PSS multilayers can reversibly bind and release transition metal ions including Fe(II), Ni(II), and Zn(II). Formation of 2-D arrays of metallo-units is achieved by μ -contact stamping transition metal salts onto the BiPE/PSS interface. Also, multilayers of BiPE are readily assembled through metal ion coordination. Due to the reversible nature of metal ion coordination, exposure of the multilayers to EDTA causes instant disassembly of the layer, a property needed to implement stimulus triggered release functions. The importance of metal ion coordination for multilayer formation is demonstrated by force-distance curves measured with AFM.

Keywords: atomic force microscopy; metal ion coordination; multilayers; μ -contact printing; thin films

Introduction

The sequential deposition of oppositely charged polyelectrolytes has become a buoyant procedure to fabricate thin films.¹ The wide spread interest in the so-called electrostatic layer-by-layer self-assembly (ELSA) method rests on the simplicity of layer formation, the excellent thickness control, and its broad applicability. Metal ions have properties that are of special interest for functional devices.^{2,3} They provide a range of binding strengths, and ligand exchange kinetics, which are needed for reversible and switchable interaction sites. The ability to interact with photons and electrons alike makes metal ion coordination compounds or metallo-supramolecular

modules (MEMOs) of particular interest as functional components in devices and materials.⁴ In addition, metal ions possess interesting magneto-optical properties that are relevant for the construction of advanced materials.⁵ Using metal ion ligand interactions in film fabrication, therefore, offers interesting perspectives including reversible interaction sites for controlled assembly and release as well as sensing.⁶ In this first account, some of the perspectives and potential features of metal ion coordination as binding motive in thin films are investigated. First, we will discuss electrostatic layer-by-layer self-assembly of BiPE with PSS and metal ion binding of the resulting multilayers, including μ -contact printing. Then, we describe a procedure to assemble multilayers through metal ion coordination and investigate the influence of metal ion–ligand interactions on the adhesion in these multilayers as determined by force-distance curves measured with AFM (Scheme 1).



Scheme 1. Structure of the bi-functional polyelectrolyte (BiPE) with bipyridine metal ion receptors and positively charged ammonium groups. The polyelectrolyte can be assembled through electrostatic interactions with negatively charged polymers, such as polystyrene sulfonate (A) as well as through metal ion coordination (B).

Experimental Section

The synthesis of BiPE and thin film assembly was performed according to literature procedures.⁷

Results and discussion

Multilayers through electrostatic interactions. The quaternary ammonium groups in BiPE provide permanent charges that open a route to fabricate multilayers through electrostatic interactions with oppositely charged polyelectrolytes, such as PSS. Multilayers are deposited onto the PEI (polyethylenimine)/PSS cushion by alternating immersion in solutions containing BiPE

and PSS and intermittent washing steps. To elucidate the internal structure the interfacial roughness, the multilayers were subjected to X-ray reflectance (XRR) measurements. Figure 1 shows a representative XRR curve of a $\text{PEI}(\text{PSS}/\text{BiPE})_3\text{PSS}$ film and the corresponding fit.

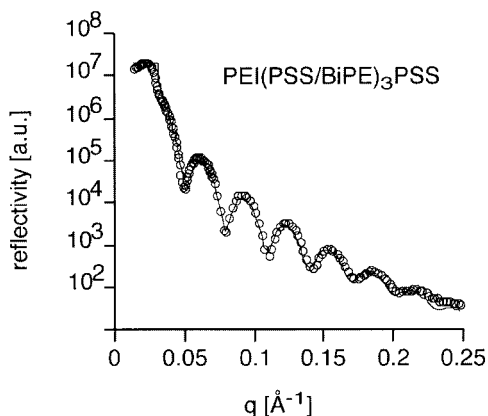


Figure 1. Representative experimental (dots) and calculated (lines) XRR curves for a $\text{PEI}(\text{PSS}/\text{BiPE})_3\text{PSS}$ multilayer (Fit parameters: electron density δ Si: $7.44 \cdot 10^{-6}$; SiO: $7.33 \cdot 10^{-6}$; film: $3.2 \cdot 10^{-6}$; thickness SiO: 0.6 nm; film: 20.5 nm; total interfacial roughness: 1 nm).

As much as seven Kiessig interference fringes are discernible, which demonstrate that the multilayer is homogeneous in thickness and composition.⁸ The detailed analysis of the reflectance curve reveals a film thickness of 20.5 nm and a roughness of approx. 1 nm. Similarly, the multilayer $\text{PEI}(\text{PSS}/\text{BiPE})_2\text{PSS}$ has a thickness of 13.4 nm. The average thickness per PSS/BiPE layer pair, therefore, amounts to 5.6 nm, or approx. 2.8 nm per layer, which is in agreement with the surface coverage determined by UV/Vis spectroscopy (not shown). Independent measurements of the thickness by optical ellipsometry confirm these results.

Metal ion coordination and exchange in PSS/BiPE multilayers. The $(\text{PSS}/\text{BiPE})_n$ multilayers can coordinate transition metal cations through the bipyridine groups. With many transition metal ions bipyridine forms octahedral tris-bipyridine complexes with the general formula $\text{M}(\text{bipy})_3$. With Fe(II) complex formation is particularly strong and gives rise to characteristic and strong metal-to-ligand-charge-transfer (MLCT) bands in the UV/Vis spectrum (Fig. 2).⁹

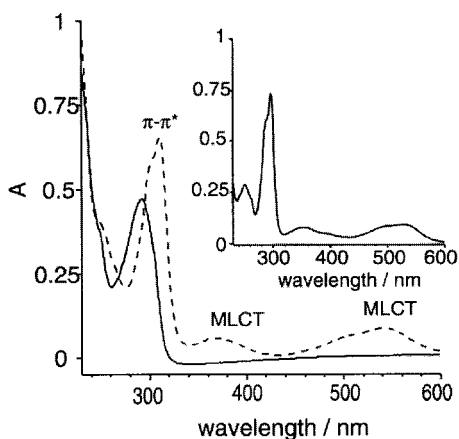


Figure 2. UV/Vis-spectra of a PEI(PSS/BiPE)₈ multilayer before (solid line) and after (dashed line) immersion in Fe(II) solution and of Fe(bipy)₃(NH₄)₂(SO₄)₂ in aqueous solution (insert).

To verify metal ion binding, the (PSS/BiPE)_n multilayer is treated with an aqueous solution containing Fe(II) ions. Figure 2 shows the UV/Vis-transmission spectrum of a PEI(PSS/BiPE)₈ multilayer before and after metal ion insertion. Initially, we observe the characteristic bipyridine transitions at 247 nm and 290 nm. After metal ion coordination, the absorption band at 290 nm shifts to 310 nm and increases in intensity. Furthermore, new bands at 371 nm and 540 nm appear, which are assigned to MLCT bands of the Fe(bipy)₃²⁺ complex. The similarity of the spectra of (PSS/Fe(II)-BiPE)₈ and Fe(bipy)₃(NH₄)₂(SO₄)₂ in solution (insert) in terms of band positions and relative intensities confirms formation of the tris-bipyridine metal ion complex in the multilayer.¹⁰

In order to demonstrate the reversibility of metal ion coordination within the multilayer, the Fe(II) containing multilayer is exposed to ethylenediaminetetraacetic acid (EDTA). In basic solution, EDTA has a strong propensity to coordinate Fe(II) (pK = 14 at pH 11).¹¹ Removal of the Fe(II) ions from the multilayer is readily confirmed by UV/Vis spectroscopy, in particular by the disappearance of the MLCT bands (not shown).

Due to the versatile coordination chemistry of bipyridine, incorporation of other metal ions, such as Ni(II) or Zn(II), in these layers give similar results. In case of Zn(II), metal ion coordination is accompanied with multilayer fluorescence (Figure 3). The similarity of the fluorescence spectra of

(PSS/Zn(II)-BiPE) and $\text{Zn}(\text{bipy})_3^{2+}$ in solution confirms as in the previous case formation of the tris-bipyridine complex.

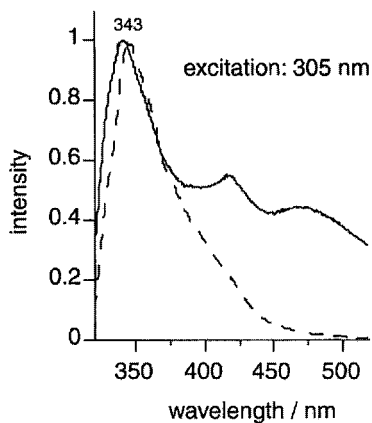


Figure 3. Normalized fluorescence spectra of a $\text{PEI}/(\text{PSS}/\text{Zn}(\text{II})\text{-BiPE})_{11}$ multilayer (solid line) and $\text{Zn}(\text{bipy})_3^{2+}$ in acetonitrile (dotted line).

Lateral patterning with metal ion coordination. The immobilization of metal ion receptors at the interface offers the possibility to confine metal ions to pre-defined areas. Lateral patterning of the surface is achieved by μ -contact stamping the transition metal salt on the (PSS/BiPE) multilayer followed by rinsing with water.

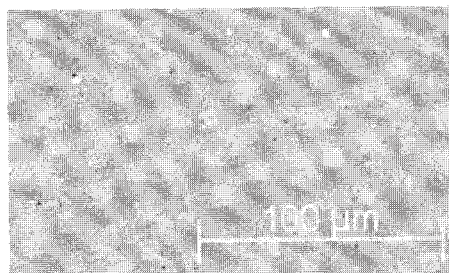


Figure 4. Phase-contrast microscopy image of a patterned $\text{PEI}(\text{PSS}/\text{BiPE})_{10}$ surface. Lateral patterning with $\text{Fe}(\text{II})$ -ions is achieved by μ -contact stamping the metal salt. The continuous dark area represents the imprinted (PSS/ $\text{Fe}(\text{II})$ -BiPE) region. (The contrast was enhanced using digital editing.)

Figure 4 shows a representative microscopy image of a quartz slide coated with 10 BiPE/PSS layers after μ -contact printing of $(\text{NH}_4)_2\text{Fe}(\text{SO}_4)_2$. The darker area in the image corresponds to regions where salt is imprinted. UV/Vis spectroscopy of the sample confirms metal-ion coordination and complex formation. We, therefore, conclude that μ -contact stamping of the transition metal salt results in spatial confinement of metallo-units. The fact that the metallo-pattern is preserved after rinsing demonstrates the high fidelity of metal ion–ligand interactions and the thereby resulting spatial confinement of the metal ions in the multilayer.

Multilayer formation with coordinative interactions. In a second approach, we explore the metal ion ligand interaction to form coordination bonds between adjacent BiPE layers. First, we generate a PEI/PSS/BiPE cushion, onto which subsequent BiPE layers are deposited through metal ion coordination. The PEI/PSS/BiPE film shows the characteristic π - π^* transition at 290 nm of the (uncoordinated) bipyridine groups.

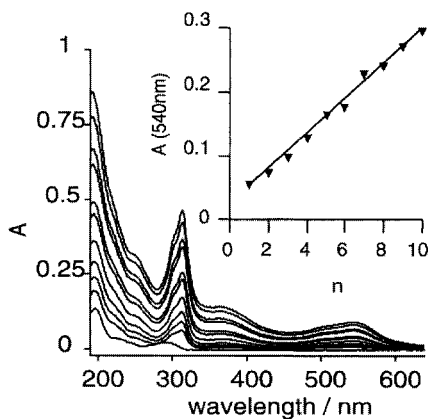


Figure 5. UV/Vis spectra of a $\text{PEI/PSS(Fe(II)-BiPE)}_n$ multilayer ($n=1-10$) on quartz substrate deposited by metal ion coordination. The bottom trace shows the π - π^* transition of uncoordinated bipyridine at 290 nm. Interlayer linkage by metal ion coordination shifts the band to 314 nm. Metal ion coordination is also confirmed by the characteristic MLCT transition at 542 nm. The insert shows the increase of absorbance at 541 nm as a function of the number of layers.

Alternating immersion of the substrate in solutions containing (a) $(\text{NH}_4)_2\text{Fe}(\text{SO}_4)_2$ and (b) BiPE

results in multilayer formation. Film growth is indicated by an increase of the MLCT bands and the π - π^* transition (Figure 5). The appearance of the MLCT band and the shift of the π - π^* transition proves metal ion coordination (*vide supra*) and formation of tris-bipyridine complexes during layer growth. The resulting multilayers are rougher than the BiPE/PSS layers, as indicated by ellipsometry, AFM and the absence of Kiessig fringes in XRR. The BiPE layers are readily disassembled by immersion in a solution containing EDTA.

Probing metal ion coordination with atomic force microscopy. The influence of metal ion coordination on the adhesion of adjacent BiPE layers is demonstrated by force-distance curves measured with AFM using a borosilicate particle in order to have a well-defined contact area. The surface of the particle is coated with a PEI/PSS/PAH/PSS/BiPE multilayer. Likewise, a silicon wafer is modified with a PEI/PSS/PAH/PSS/BiPE multilayer. Both interfaces are terminated with BiPE to facilitate metal ion coordination upon contact of the particle modified AFM tip and the surface. Force-distance curves are measured in aqueous solution containing 10 mM NaCl.

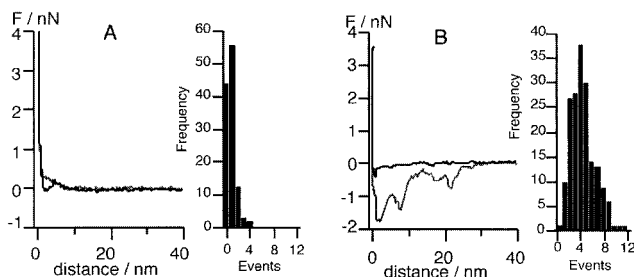


Figure 6. Exemplary force distance curve before (A) and after (B) incubation of the sample in a 0.1 M NiCl_2 solution measured in 10 mM NaCl. The histograms show the distribution of the adhesion events.

A representative force-distance curve in the absence of transition metal ions is shown in Figure 6 (A). At large separation between the two surfaces there is no physical interaction and as a result no change in the cantilever position. During the approach of the tip we observe a long-range repulsive force between the interfaces, which is attributed to electrostatic interactions causing the cantilever to bend. Upon withdrawal we observe no or very little attractive interactions between the two surfaces, which are attributed to unspecific steric and electrostatic interactions of possibly entangled polyelectrolytes under the influence of the applied force during the approach. To

examine the influence of metal ion coordination, the silicon wafer is immersed in a solution containing 0.1 M NiCl_2 . After rinsing the wafer with water we record another force-distance curve. A typical example is shown in Figure 6 (B). We notice a short-range attractive interaction during the approach of the tip to the surface, which causes the cantilever to bend. Upon withdrawal of the tip we observe several rupture events, which are attributed to metal ion ligand as well as electrostatic interactions between the two interfaces. We interpret this observation as follows. The metal ions yield a binding force between the two interfaces through metal ion coordination. Most likely, binding results predominantly through ligand exchange reactions because the interface was rinsed with water after metal ion deposition. If we assume that metal ion coordination is much stronger than electrostatic interactions, withdrawal of the tip will first pull apart and stretch the crosslinked polyelectrolyte network between the two interfaces until eventually the metal ion ligand bonds begin to rupture. As a result, the rupture events in the force-distance curves are generally broad typical for elastically deformable connected networks. The overall procedure is repeated for a defined number of experiments and added together, yielding a histogram. We show the number of rupture events for repeated approach-withdrawal cycles at one spot on the surface. Clearly, the presence of NiCl_2 has a profound influence on the number and distribution of rupture events. Therefore, we conclude that the attractive interactions revealed in the force-distance curves result from multiple interactions including electrostatic interactions of entangled polyelectrolytes as well as metal ion coordination. With this procedure we, therefore, measure the overall adhesion between the two interfaces. Clearly, the attractive interactions observed in the presence of transition metal ions confirm the importance of metal ion coordination to the formation of the multilayers.

Conclusions

We present a versatile and modular approach to incorporate metallo-units into thin films. A polyelectrolyte (BiPE) is employed that has permanent positive charges and metal ion receptors. Transition metal ions can be incorporated into the BiPE/PSS multilayers either by adsorption from solution or μ -contact stamping. The latter approach results in spatially confined regions of metallo-units. Through a competing complexing agent, such as EDTA, the metal ions are removed from the film. Multilayer formation is also possible by metal ion coordination between layers. Film growth is linear, however, the resulting interface is not as smooth as that of the

ELSA multilayers. The quality of these metal ion coordinated LbL films can be improved in several ways, including the length of the polymer, the reversibility of metal ion coordination, and the assembly protocol. Strong binding between layers through metal ion coordination is confirmed by force-distance curves measured by AFM. The presence of metal ions has a profound influence on the number of rupture events. Although it is not possible with this approach to investigate single interactions it is possible to study the overall effect of strong interactions, such as metal ion coordination, because the receptors are firmly attached through multiple bonds to the underlying substrate. These metal ion coordinated layers readily disassemble upon exposure to EDTA, which opens interesting opportunities to controlled release applications. While our initial purpose was meant as a proof of principle it became clear at the end of this study that metal ion coordination adds a rich flavor to ELSA multilayers in terms of fabrication, characterization, and function.

Acknowledgement. Financial support through the Deutsche Forschungsgemeinschaft is greatly appreciated. Helmuth Möhwald is acknowledged for valuable discussions. The authors especially thank Christa Stolle for the synthesis of the compounds. Hauke Schollmeyer is acknowledged for performing the X-ray experiments.

¹ Decher, G. *Science* **1997**, 277, 1232–1237.

² Holliday B. J.; Mirkin C. *Angew. Chem. Intern. Ed.* **2001**, 40, 2022–2043.

³ Kurth, D. G. *Annals of the New York Academy of Sciences* **960** (2002) 29–39.

⁴ Schütte, M.; Kurth, D. G.; Linford, M. R.; Cölfen, H.; Möhwald H. *Angew. Chem. Int. Ed.* **1998**, 37, 2891–2893.

⁵ Gutlich, P.; Hauser, A.; Spiering, H. *Angew. Chem. Intern. Ed.* **1994**, 20, 2024–2054.

⁶ Liu, S.; Kurth, D. G.; Möhwald, H.; Volkmer D. *Adv. Mater.* **2002**, 14, 225–228.

⁷ Krass, H.; Papastavrou, G.; Kurth, D. G. *Chem. Mater.* **2003**, 15, 196–203.

⁸ Kiessig, H. *Ann. d. Physik* **1931**, 10, 769–788.

⁹ Constable, E. C. *Advances in Inorganic Chemistry*, **1989**, 34, 1–63.

¹⁰ Bryant, G. M.; Fergusson, J. E.; Powell, H. K. *J. Aust. J. Chem.* **1971**, 24, 257–273.

¹¹ Jander Blasius, *Einführung in das anorganisch-chemische Praktikum*, 12. Auflage, S. Hirzel Verlag: Stuttgart **1987**, p 323.

